The Role of Nitrogen on the Mechanical Properties of the Novel Carbon Nitride Nanothreads

Zhuoqun Zheng[1,2], Haifei Zhan[2,], Yihan Nie[2], Xu Xu[1,**], and Yuantong Gu[2]*

[1]College of Mathematics, Jilin University, 2699 Qianjin Street, Changchun, 130012, China

[2]School of Chemistry, Physics and Mechanical Engineering, Queensland University of Technology (QUT), Brisbane QLD 4001, Australia

Abstract

Carbon nanothread (C-NTH) is a new ultrathin one-dimensional sp^3 carbon nanostructure, which exhibits promising applications in novel carbon nanofibers and nanocomposites. Recently, researchers successfully a new alternative structure - ultrathin carbon nitride nanothread (CN-NTH). In this work, we investigate the mechanical properties of CN-NTHs through large-scale molecular dynamics simulations. Comparing with their C-NTH counterparts, CN-NTHs are found to exhibit a higher tensile and bending stiffness. In particular, due to the bond re-distribution, the CN-NTHs in the polymer I group and tube (3.0) group are found to possess a higher failure strain than their C-NTH counterparts. While, the CN-NTH in the polytwistane group has a smaller failure strain compared with the pristine C-NTH. According to the atomic configurations, the presence of nitrogen atoms always leads to stress/strain concentrations for the nanothreads under tensile deformation. This study provides a comprehensive understanding of the mechanical properties of carbon nitride nanothreads, which should shed lights on their potential applications such as fibers or reinforcements for nanocomposites.

* Corresponding author. Email: zhan.haifei@qut.edu.au (Haifei Zhan)
** Corresponding author. Email: xuxu@jlu.edu.cn (Xu Xu)

1. Introduction

Carbon-based nanostructures have been extensively studied due to their intriguing chemical and physical properties and promising applications. To date, different carbon-based nanostructures have been experimentally synthesized, such as fullerenes, carbon nanotube (CNT), and graphene.[1-3] Recently, a new class of ultra-thin one-dimensional (1D) carbon nanostructure - carbon nanothread (C-NTH) has been successfully synthesized through the slow solid-state reaction of benzene (under high-pressure).[4] C-NTH has a close-packed *sp*^{3}-bonded structure, which has been firstly predicted in 2001 with a high Young's modulus exceeding 1.5 TPa and a very large insulating band gap based on density functional theory (DFT).[5] Following this initiative, continuing efforts have been devoted to explore the C-NTH based on both theoretical[6] and experimental studies.[7] According to the theoretical calculations, there are many different types of stable C-NTH structures, including the "degree-6"[8] and "degree-4"[9] nanothreads, which also include the previously proposed *sp*^{3} nanothreads, i.e., tube (3,0),[5] polymer I,[9] and polytwistane.[7, 10] Continuing experimental efforts have been devoted to characterize the atomic structures of the carbon nanothreads by using different techniques, e.g., based on high-resolution transmission electron microscopy,[11] and through advanced solid-state nuclear magnetic resonance experiments.[12]

To date, extensive computational works have been conducted to investigate the properties of C-NTHs and explore their applications. It is found that the C-NTHs exhibit remarkable mechanical properties. DFT calculations show that the theoretically predicted nanothreads have a wide range of Young's modulus ranging from 0.08 to 1.16 TPa.[8] Molecular dynamics (MD) simulations reveal that the C-NTH has a high tensile stiffness comparable with that of CNT (i.e., around 850 GPa), and its yield strain is approximately 14.9% with an ultimate stress of about 143.3 GPa. Our recent works show that the yield strength of C-NTH is almost independent of the constituent unit cells, and the failure behavior is controlled by its structure.[13] In particular, the C-NTH with the so-called Stone-Wales transformation defects exhibits a tunable ductility. Studies also shown that the mechanical properties of C-NTH are heavily dependent on their morphology, temperature[13] and hydrogenation states.[14] Besides the mechanical properties, researchers also found that C-NTH possesses a tailorable thermal transport properties.[15-16] These excellent properties of different nanothreads make them promising building blocks for nanofibers,[17] composite reinforcements[18] and nano-sized mechanical resonators.[19]

Based on the theoretical predictions, nanothreads are chemically versatile,[20-21] i.e., they can be formed from heteroaromatic molecules like aniline[22], pyridine[21, 23] and other aromatic compounds.[21] Recent study shows that slow compression and decompression of polycrystalline pyridine allows for the formation of single crystal of carbon nitride nanothreads (CN-NTH), with an empirical formula of C_5NH_5.[23] Given the intriguing properties of C-NTHs, it is of great interests to explore the mechanical behaviors of CN-NTH.

Recent DFT calculation reveals the outstanding mechanical properties of partially saturated C- and CN-NTHs.[24] However, the mechanical behaviors of fully saturated CN-NTHs remains unclear, which becomes the focus of this work. For such purpose, we conduct a series of *in silico* studies to explore the mechanical behaivors of CN-NTHs. It is found that the CN-NTHs exhibit higher tensile and bending stiffness compared with C-NTHs, and the polymer I type and tube (3,0) type CN-NTHs even exhibit a higher failure strain.

2. Materials and Methods

The mechanical properties of the CN-NTHs were assessed through large-scale MD simulations. The ReaxFF potential was adopted to depict the atomic interactions between C-C and C-N atoms.[25] ReaxFF is an empirical bond-order-dependent potential that allows for fully reactive MD simulations of chemical reactions, including bond rupture during the mechanical loads. The parameters are derived from quantum chemistry calculations. To note that for carbon-based nanostructures, the adaptive intermolecular reactive empirical bond order (AIREBO) potential has been frequently employed to probe their mechanical properites.[26-27] However, current AIREBO is lacking of atomic interactions between C and N and is unable to describe the atomic interactions in the carbon nitride nanothread. Thus, we adopted the ReaxFF potential to describe the carbon nitride naonthread as previous studies have successfully applied ReaxFF to investigate the mechanical properties of various carbon nanostructures, such as tensile properties of carbon nanothread,[14, 28] ballistic fracture of CNTs,[29] and mechanical[30] and thermal properties[31] of graphene or graphene derivatives.

The initial structures of CN-NTHs were optimized by the conjugate gradient algorithm, and then equilibrated under isothermal-isobaric ensemble (constant atoms number, constant temperature and constant pressure) by using Nosé-Hoover thermostat[32-33] for 500 ps. After relaxation, a low temperature of 10 K was adopted in order to limit the thermal influence. A quasi-static tensile scheme was applied, i.e., the sample was stretched under a low tensile velocity (0.014 Å/ps, corresponding to an effective strain rate of 10^{-7} fs^{-1}), and relaxed for 20 ps for every 0.1% strain increment. The tensile load was applied to one end of the structure, with the other end being fixed. A time step of 0.5 fs was used, and non-periodic boundary conditions were applied in the axial direction of the nanothreads. All simulations were performed by using the open-source code Large-scale Atomic/Molecular Massively Parallel Simulator (LAMMPS).[34]

During the tensile simulation, the tensile force and the commonly used virial stress were calculated. The virial stress is defined as[35]

$$\Pi^{\alpha\beta} = \frac{1}{\Omega}\left\{-\sum_i m_i v_i^{\alpha} v_i^{\beta} + \frac{1}{2}\sum_i \sum_{j\neq i} F_{ij}^{\alpha} r_{ij}^{\beta}\right\} \quad (1)$$

Here, Ω is the volume of the system; m_i and v_i are the mass and velocity of atom i; F_{ij} and r_{ij} are the force and distance between atoms i and j; and the indices α and β represent the Cartesian components. The

volume of the nanothread is estimated by approximating an individual nanothread as a solid cylindrical beam with an effective diameter of 5 Å.[28] Adopting different approaches to calculate the volume of the nanothread bundle would lead to different absolute stress values but not affect their relative magnitudes. The atomic virial stress was estimated according to Eq. 2 as

$$\pi_i^{\alpha\beta} = \frac{1}{\overline{\omega_i}}\left\{-m_i v_i^{\alpha} v_i^{\beta} + \frac{1}{2}\sum_{j\neq i} F_{ij}^{\alpha} r_{ij}^{\beta}\right\} \quad (2)$$

where $\overline{\omega_i}$ represents the effective volume of atom i and $\Omega = \sum \overline{\omega_i}$.

3. Results and Discussion

Three groups of N-NTHs as reported by Li *et al.*[23] have been investigated as shown in **Figure 1**. For comparison purpose, the mechanical properties of the corresponding carbon nanothread counterparts are also re-visited, including the polymer I,[6] polytwistane,[10] and tube (3,0), denoted as C-NTH_a, C-NTH_b and C-NTH_c, respectively. Depending on the locations of the nitrogen atoms, there are two types of carbon nitride nanothreads (CN-NTH_a1 and CN-NTH_a2) for the polymer I group (Figure 1a); one type of carbon nitride nanothreads (CN-NTH_b) for the polytwistane group (Figure 1b); and two types of carbon nitride nanothreads (CN-NTH_c1 and CN-NTH_c2) for the tube (3,0) group (Figure 1c). A similar sample length (excluding the two edges) around 14 nm are considered for all nanothreads for the tensile simulation.

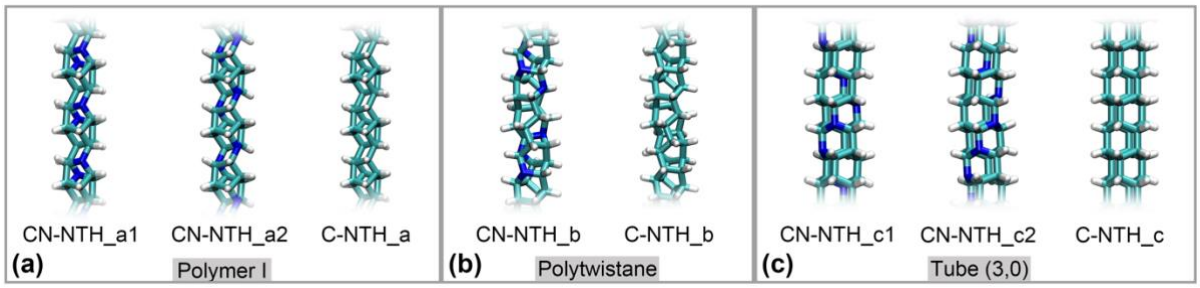

Figure 1. Atomic configurations of the carbon nitride nanothreads (CN-NTHs) and the corresponding carbon nanothread (C-NTH) counterparts. (a) The polymer I group; (b) The polytwistane group; and (c) The tube (3,0) group. Blue, cyan and white colors represent the nitrogen, carbon and hydrogen atoms, respectively.

3.1 Tensile characteristics of carbon nitride nanothreads

Figure 2 shows the tensile force-strain curves of all CN-NTHs. Here, the engineering strain is calculated, i.e., $\varepsilon = \Delta L/L_0$ (with ΔL and L_0 as the length change and the initial length of the structure). In general, the force increases continuously and then experiences a sudden drop when the strain reaches the threshold value, indicating a brittle tensile characteristic as observed in the C-NTHs from both MD simulations,[28, 36-37] and DFT calculations.[23, 38] According to the atomic configurations, bond breaking is observed when the strain passes the threshold value. As such, the force and strain at the threshold point are regarded as the critical force and failure strain, respectively. Comparing with the C-NTHs, nitrogen atoms

are found to induce different influences on the tensile properties of the nanothreads. For the polymer I (Figure 2a) and the tube (3,0) group (Figure 2c), the nanothreads with nitrogen are found to possess a higher failure strain and critical force than their carbon nanothread counterparts. For instance, the failure strains for CN-NTH_c1 and CN-NTH_c2 are about 22.5% and 25.4%, respectively, and their critical forces are around 22.2 nN and 22.8 nN, respectively. In comparison, the C-NTH_c shows a failure strain of about 20.5% and a critical force of 19.8 nN. Opposite from these two groups, the carbon nitride nanothread in the polytwistane group exhibits a smaller failure strain and critical force than that of the carbon nanothread (Figure 2b).

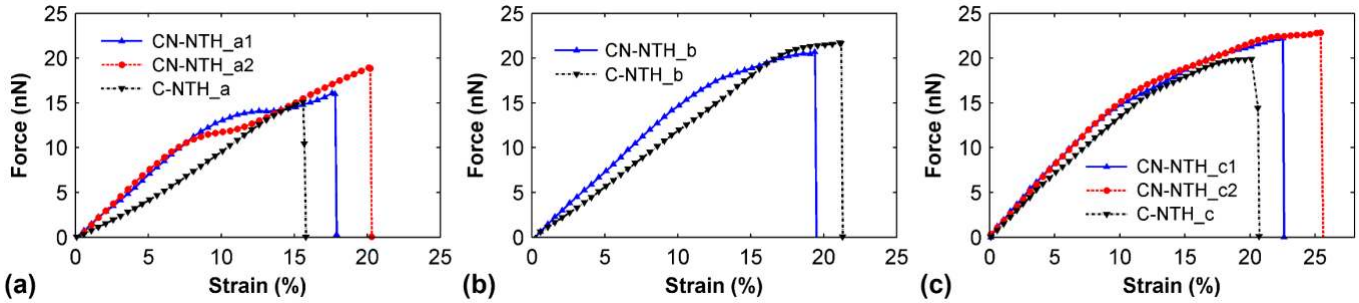

Figure 2. The tensile force as a function of strain for CN-NTHs and C-NTHs. (a) The polymer I group; (b) The polytwistane group; and (c) The tube (3,0) group.

It is uniformly found from Figure 2 that the gradients of the force-strain curves for CN-NTHs are larger than that of the C-NTHs, signifying a higher tensile stiffness or modulus. Following the solid cylinder approximation with a diameter of 0.5 nm,[28] the tensile force can be converted to the engineering stress, i.e., $\sigma = F/A_{eff}$ (Here, A_{eff} is the effective cross-sectional area). In this regard, the effective tensile stiffness can be estimated from the stress-strain curve based on the assumption of linear elasticity (for the strain ranging from 0% to 4%). Basically, the tube (3,0) group exhibits the highest tensile stiffness, which is around 742 GPa, 865 GPa, and 842 GPa for CN-NTH_c, CN-NTH_c1, and C-NTH_c2, respectively. In the polymer I group, the carbon nanothread exhibits a low tensile stiffness of around 383 GPa, which is nearly doubled for the structure with nitrogen, i.e., around 688 GPa for CN-NTH_a1 and 739 GPa for CN-NTH_a2. Similarly, in the polytwistane group, the tensile stiffness is around 737 GPa for CN-NTH_b, more than 30% higher than its counterpart C-NTH_b (about 546 GPa).

Above results suggest that the presence of nitrogen introduces a remarkable impact to the tensile properties of the nanothread. Such observation is divergent from the earlier DFT calculations on pyridine-derived nanothread (the tube(3,0) nanothread)[38] and partially saturated carbon nitride nanothreads,[23] from which a minor influence is resulted from the presence of N (with a slight increase in tensile stiffness). Although it is beyond the scope of the current work to exploit in-detail the underlying reasons for such

discrepancy, there are several expected influential factors such as structural influence, sample length, and thermal influence. For instance, the atomic structures in earlier DFT calculations[23, 38] are different from the structures investigated in this work. The distribution of N atoms is expected to affect the stress or strain distribution, which could thus lead to different influences for different nanothread structure as seen in Figure 2. In addition, the applied empirical potentials can also result in certain discrepancy. As mentioned earlier, this work employed the ReaxFF potential to represent the atomic interactions within the nanothread. There are many different ReaxFF parameterizations for C-H-N system, while none of them is specifically developed for nanothread. In this work, we have examined 11 different ReaxFF potentials and find that these potentials can lead to very divergent results even for the pristine carbon nanothreads (see **Supporting Information S1**). The ReaxFF parameterization selected in this work can produce consistent results with varying simulation settings as further discussed below. It has been shown that ReaxFF usually overestimate the fracture properties of nanothreads,[36] and an adequate re-parameterization of the potential could improve the accuracy of the prediction from the MD simulations.

Overall, carbon nitride nanothreads exhibit a same brittle characteristic as their carbon counterparts, but they show a larger tensile stiffness, and the impacts from the nitrogen on the critical force or failure strain is dependent on the structure of the nanothreads. To further affirm such observation, we conduct three groups of simulations under three different simulation conditions by taking CN-NTH_a1 and CN-NTH_a2 as representative structures. The first group examines the effective tensile strain rate ranging from 1×10^{-8} fs^{-1} to 1×10^{-6} fs^{-1}. The second group considers the tensile deformation of the nanothreads from different initial status, i.e., after a relaxation time of 500 ps, 750 ps, 1750 ps, and 2750 ps. The third group adopts a sample length ranging from 2 to 16 nm. It is found that the examined strain rate, sample length, and the initial status exert ignorable influence on the tensile behaviors of the CN-NTHs (see **Supporting Information S2** for detail results).

It is worthy to note that this study has adopted a low temperature of 10 K, which is also commonly applied in literature when investigating the mechanical properties of nanomaterials in order to remove the thermal influence. According to literature, the elastic limit or failure strain normally experiences a nontrivial decrease when the temperature increases.[13-14, 36] That is, the relatively high failure strains in Figure 2 are likely to overestimate the behavior of actual nanothreads at room temperature. As an evidence, we compare the tensile deformation of CN-NTH_a1 and CN-NTH_a2 under the temperature of 10 K, 50 K, 100 K, 200 K, and 300 K. According to **Figure 3**, the nanothreads exhibit earlier failure at a higher temperature. For instance, the failure strain for CN-NTH_a1 decreases from ~17.8% (at 10 K) to ~11.9% (at 300 K). Due to the complexity raised by the thermal influence, a future study is needed to investigate

the influence of temperature on the mechanical properties of CN-NTH, which is beyond the scope of the current work. In this study, a low temperature of 10 K has been adopted. This is also commonly applied in literature when investigating the mechanical properties of nanomaterials in order to remove the thermal influence.

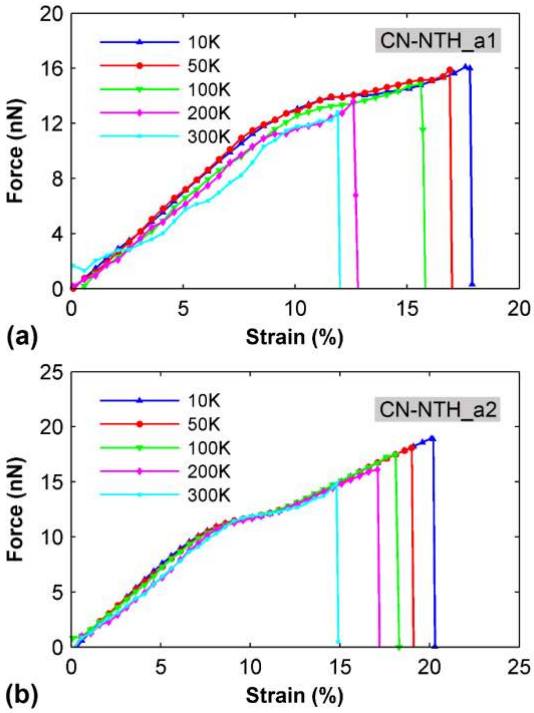

Figure 3. The influence of temperature on the tensile properties of carbon nitride nanothreads. (a) The CN-NTH_a1; and (b) The CN-NTH_a2.

3.2 The tensile deformation process

To exploit the role of nitrogen, we first compare the radial distribution function (RDF) of the carbon bonds between C-NTH and CN-NTH. Here, the RDF is calculated from a relaxation simulation under isothermal-isobaric ensemble with a duration of 500 ps. As illustrated in **Figure 4**, the RDF for C-NTHs exhibit a single peak, signifying a uniform C-C bond length within the structure. In comparison, the CN-NTHs show a remarkably different RDF pattern. For instance, three peaks can be identified for CN-NTH_c2 that are corresponding to the C-C bonds in the tube(3,0) group (Figure 4c). These results indicate that the C-C bond length is no longer uniform when nitrogen is introduced. Specifically, the CN-NTHs in polymer I and tube (3,0) groups exhibit different RDF profiles, implying that the influence on the C-C bond length from nitrogen atoms also varies with their location.

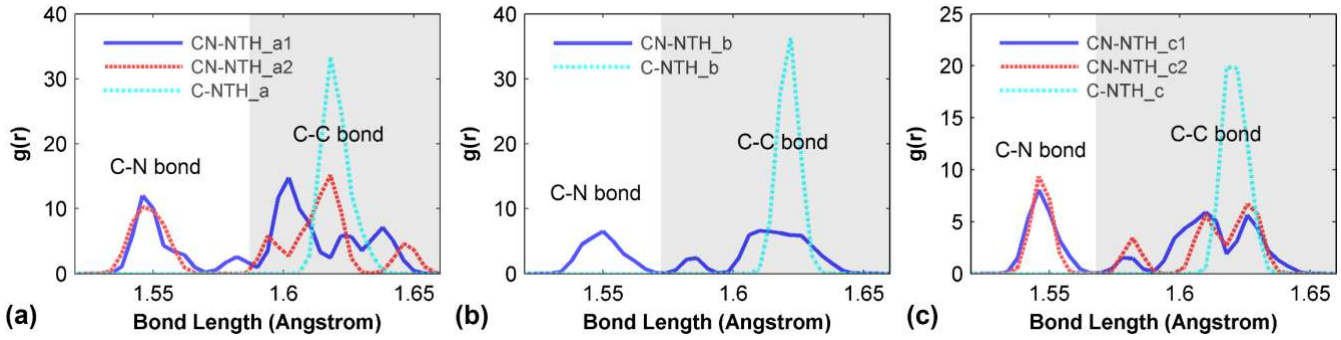

Figure 4. The radial distribution function (RDF) of the C-N and C-C bonds of the nanothreads. (a) The polymer I group; (b) The polytwistane group; and (c) The tube (3,0) group.

With this understanding, we then analysis how the covalent bonds change with the tensile deformation, which reflects the deformation process of the nanothreads. For such purpose, we divide the C-C and C-N bonds into different groups based on the structure of the nanothreads, the bond length distribution and their stress distribution status under tensile deformation. For C-NTH_a, the RDF of the bond length at a tensile strain of 10% (see **Supporting Information S3**) suggests that the carbon bonds can be classified into three groups as illustrated in the left panel of Figure 5a, denoted as CC1, CC2 and CC3. Following such classification approach, the presences of nitrogen atoms will result in different C-N bond groups in the polymer I group. For CN-NTH_a1, the location of the two nitrogen atoms in a unit cell will lead to three C-N bond groups (middle panel of Figure 5a), while there are only two C-N bond groups in CN-NTH_a2 (right panel of Figure 5a). The percentages of each bond group is listed in Table S2 in Supporting Information S3.

Figure 5b, 5c and 5d compare how different groups of covalent bonds response to the tensile deformation for nanothreads in the polymer I group. Here, the averaged bond length change ΔL_b^{ave} is tracked, which is calculated based on the bond length change in each group. The positive and negative bond change indicate the occurrences of bond stretching and compression, respectively. Overall, the stretched bonds (for both C-C and C-N bonds) show a gradual increase when the tensile strain is within approximately 5%, after which, a significant increase is observed. These results indicate that the bond stretching plays an ignorable role during the initial tensile deformation of the nanothreads. According to the atomic configurations, the polymer I group has a zigzag morphology and it can be taken as constructed purely from the so-called Stone-Wales transformation (SWT) defects.[28] During the initial deformation, the stretching of the whole structure is majorly accommodated by the increase of bond angles at the SWT defects. As evidenced from the trajectory of the bond length and bond angle at the SWT defects for the C-NTH_a (see **Supporting Information S4**), the bond length experiences insignificant change until the strain is larger than around 7%, while the bond angle increases continuously from the beginning of the tensile deformation.

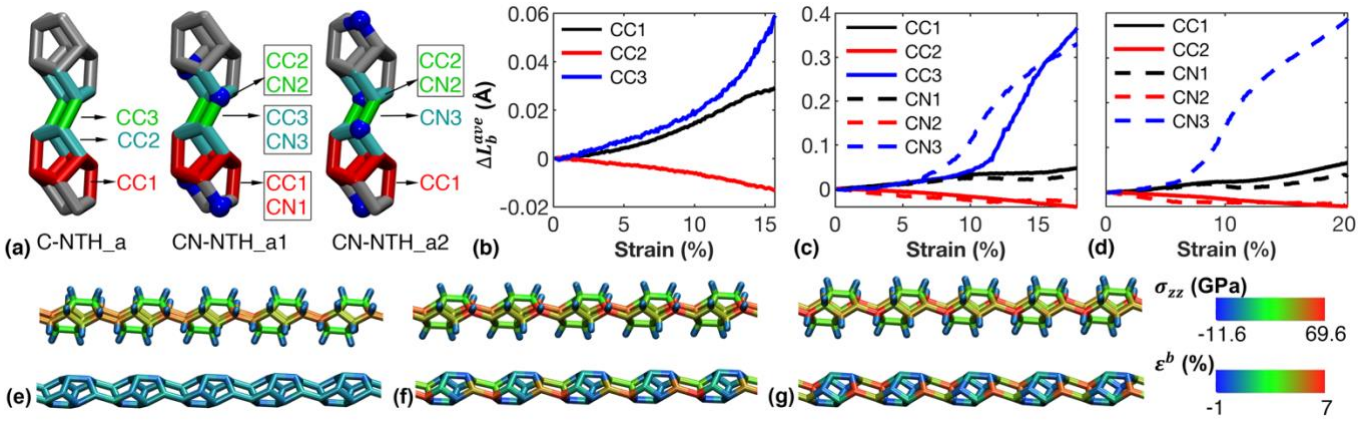

Figure 5. Tensile deformation of the nanothreads in the polymer I group. (a) The C-C and C-N bond groups in C-NTH_a, CN-NTH_a1, and CN-NTH_a2, respectively; The average bond length change in each bond group as a function of tensile strain for: (b) C-NTH_a; (c) CN-NTH_a1; and (d) CN-NTH_a2. The curves are truncated at the failure strain; The stress distribution (upper panel) and strain distribution (lower panel) at the tensile strain of 15% (before failure) for: (e) C-NTH_a; (f) CN-NTH_a1; and (g) CN-NTH_a2. The atomic configuration is a section of the whole sample.

According to Figure 5b, the carbon bonds in both CC1 and CC3 group experience stretching while the CC2 group experiences compression during tensile deformation of C-NTH_a. Specifically, carbon bonds in CC3 undergo the largest stretching. Such deformation process is well reflected by the atomic configurations in Figure 5d, from which the stress and strain concentration is observed in the carbon bonds in CC3 group. With further deformation, the failure is also occurred in CC3 group. Here, the atomic strain is just a placeholder for the continuum strain, which is defined as $\varepsilon_a = \sum_M \varepsilon_i^b / M$, where, $\varepsilon^b = (b_d - b_0)/b_0$ is the bond length changing ratio, and b_0 and b_d represent the initial and deformed bond length, respectively. M is the number of bonds for the corresponding atom. From Figure 5c and 5d, the presence of nitrogen does not alter the pattern of the stress distribution, i.e., C-N bonds share the same changing tendency with the C-C bonds in the same group. It is seen from Figure 5c that both CC3 and CN3 experience a large extension for CN-NTH_a1 under tensile deformation, while only CN3 shows a large bond stretch in CN-NTH_a2. Different from the C-C bonds in C-NTH_a, the C-N bonds are able to bear much larger stretch before failure, e.g., approaching 0.4 Å. Such observation explains why CN-NTH_a2 shows the highest failure strain but C-NTH_a exhibits the lowest failure strain in Figure 2a. According to Figure 5e to 5g, the C-C bonds in CC3 group or C-N bonds in CN3 group experience the highest stress/strain, which initiate the failure when the tensile strain reaches the failure point.

In the polytwistane group, the backbone structure of the nanothreads is the CNT(2,1).[7] According to the atomic configuration in Figure 6a, the C-C bonds in C-NTH_b can be classified into three groups based on their location along the axial direction, including CC1, CC2 and CC3. Similarly, the presence of

nitrogen will introduce three C-N bond groups. The tensile deformation of the C-NTH_b is dominated by the stretching of C-C bonds in the CC1 group, while the other two groups are found to under compression (especially CC3, Figure 6b). Such trend is also observed from the tensile deformation of the CN-NTH_b in Figure 6c. According to the atomic configurations in Figure 6d, the stress or strain is evenly distributed in C-NTH_b. In comparison, the existence of nitrogen results in stress/strain concentration in the nanothreads, which initiate the failure with further tensile deformation.

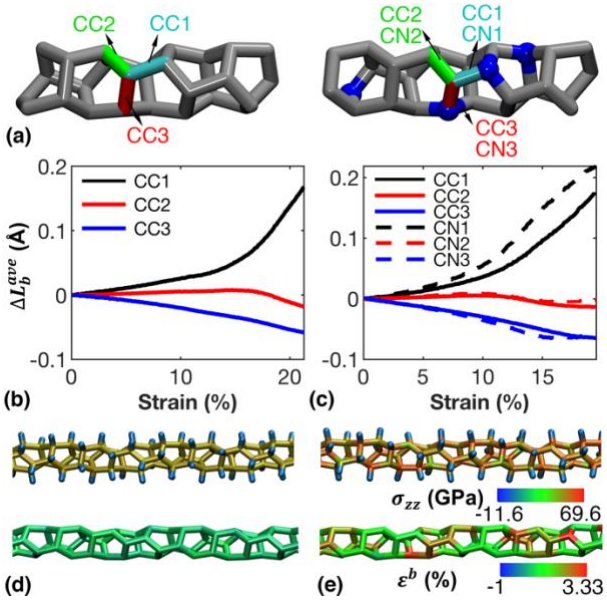

Figure 6. Tensile deformation of the nanothreads in the polytwistane group. (a) The C-C and C-N bond groups in C-NTH_b, and CN-NTH_b, respectively; The average bond length change in each bond group as a function of tensile strain for: (b) C-NTH_b; and (c) CN-NTH_b. The curves are truncated at the failure strain; The stress distribution (upper panel) and strain distribution (lower panel) at the tensile strain of 15% (before failure) for: (d) C-NTH_b; and (e) CN-NTH_b. The atomic configuration is a section of the whole sample.

For the tube (3,0) group, the C-C bonds can be classified into two groups, i.e., CC1 and CC2 (Figure 7a). The introduction of nitrogen will thus lead to two C-N bond groups, i.e., CN1 and CN2. Before the tensile deformation, the C-C-bonds have a uniform length for the C-NTH_c as illustrated in Figure 4c. However, during the tensile simulation, the CC1 group experiences stretch and the CC2 group is under compression as shown in Figure 7b. The absolute bond length change in CC1 group is much larger than that in CC2 group. In other words, there is a tensile stress/strain concentration in CC1 group. To note that Figure 7e is unable to show the bond stress concentration as it is colored based on the atomic stress or strain, and the atoms are geometrically equivalent to each other. Similar as the nanothreads in polymer I group and polytwistane group, the C-N bonds in the CN group follows the same stress status as the corresponding CC group. As compared in Figure 7c and 7d, the C-N bonds in CN1 group experience stretch and the C-N

bonds in CN2 group experience compression. It is interesting to note that the C-C bonds in the nanothreads with nitrogen can bear larger stretch before the eventual failure. For instance, the average C-C bond length change in CC1 group is around 0.17 Å for C-NTH_c, which increases to 0.27 Å for CN-NTH_c1 and 0.35 Å for CN-NTH_c2. The increased extensibility of the C-C bonds is resulted from the re-distribution of the C-C bond length due to the presence of nitrogen as indicated in Figure 4c. According to the atomic configurations (Figure 7d and 7e), the nanothreads with nitrogen exhibit a strong stress/strain concentration at the location of the nitrogen atoms. For all structures, the failure is found to initiate in the CC1 group.

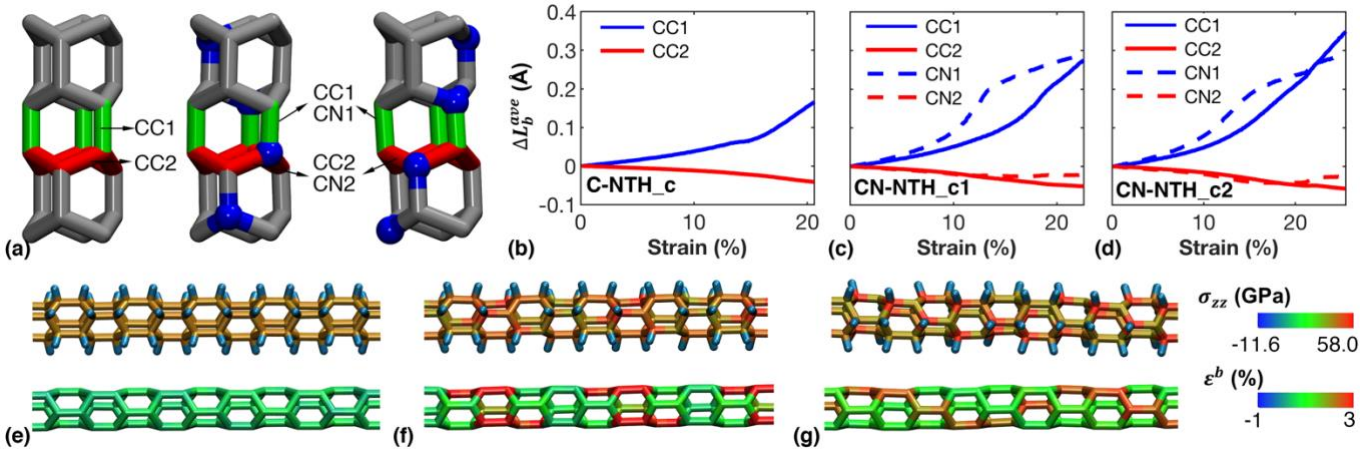

Figure 7. Tensile deformation of the nanothreads in the tube (3,0) group. (a) The C-C and C-N bond groups in C-NTH_c, CN-NTH_c1, and CN-NTH_c2, respectively; The average bond length change in each bond group as a function of tensile strain for: (b) C-NTH_c; (c) CN-NTH_c1; and (d) CN-NTH_c2. The curves are truncated at the failure strain; The stress distribution (upper panel) and strain distribution (lower panel) at the tensile strain of 15% (before failure) for: (e) C-NTH_c; (f) CN-NTH_c1; and (g) CN-NTH_c2. The atomic configuration is a section of the whole sample.

3.3 The bending stiffness

With above understanding, we also assess the flexibility of CN-NTHs to further understand their mechanical characteristics. It is a challenge to calculate the bending stiffness or flexural rigidity of CN-NTH due to its ultra-thin diameter and the non-smooth surface. As such, we employ the free vibration test to estimate the bending stiffness, which is commonly used to probe the dynamic mechanical properties of 1D nanostructures[19, 39-42] or 2D nanoribbons.[43-46] The free vibration of the nanothreads is triggered by applying a sinusoidal velocity excitation $v(z) = a\sin(\pi z/L)$ along the length of the structure, where $a =$ 2 Å/ps is the actuation amplitude. A small time step of 0.1 fs is used for the vibration test, and the examined nanothreads have a length of about 10 nm (excluding the two fixed edges). The vibration simulation has been continued for 500 ps. The CN-NTHs in the polymer I group are considered as the representative nanothreads.

Figure 8a shows a representative time history of the external energy (EE) of CN-NTH_a1 during the free vibration. Here, EE is defined as the difference in the potential energy before and after the transverse velocity actuation is applied to the nanothreads. Based on the fast Fourier transform (FFT),[47] the natural frequency can be extracted from the EE trajectory. As illustrated in Figure 8b, two frequency components can be resolved (~105.0 GHz and ~159.9 GHz), which correspond to two natural frequencies of about 52.5 GHz and 80.0 GHz, respectively. According to the trajectory of the center of mass of the nanothread, the vibration is decomposed along two lateral directions with different frequencies, which is similar as observed in the metallic and silicon nanowires in our previous works[40-41] (See **Supporting Information S5** for details). Such results indicate the anisotropic nature of the nanothreads, which are also observed in the examined C-NTH_a and CN-NTH_a2 (see **Supporting Information S6**).

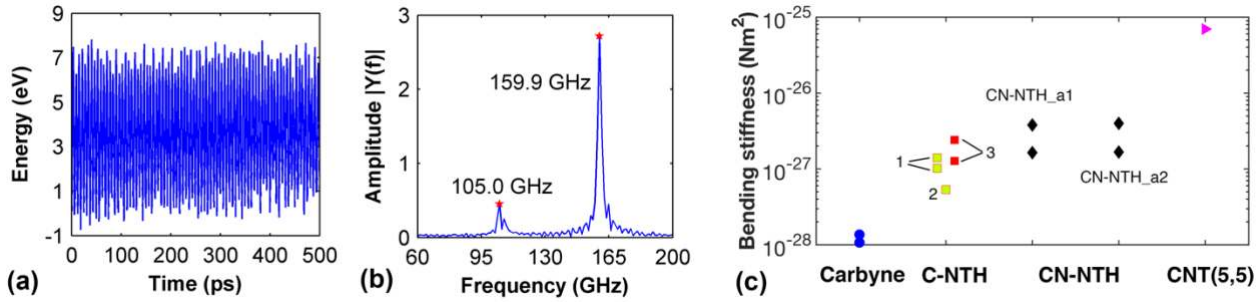

Figure 8. Bending stiffness of CN-NTH. (a) The time history of the external energy of CN-NTH_a1 under free vibration; (b) The corresponding frequency spectrum obtained from FFT analysis; and (c) Bending stiffness of different 1D carbon materials, including carbyne,[48] C-NTH (1 – Ref.,[13] 2 – Ref.,[28] 3 – this work), CN-NTH_a1, CN-NTH_a2, and CNT(5,5).[28]

Approximating the nanothread as a continuum beam, the bending stiffness (EI) can be estimated from the Euler-Bernoulli beam theory, i.e., $f = \frac{\omega}{2\pi L^2}\sqrt{EI/\rho A}$. Here, f is the vibration frequency; ω is the eigenvalue calculated from the characteristic equation ($\omega = 4.43$ for a beam with doubly clamped boundary conditions); L is the sample length; A is the cross-sectional area; and ρ is the mass density. According to the frequency spectrum, the bending stiffness for C-NTH_a is 1.27×10^{-27} N·m^2 and 2.42×10^{-27} N·m^2 in the two vibration directions, respectively, which agrees well with that estimated from the bending simulation.[13] It is surprisingly found from Figure 8c that CN-NTH_a1 and CN-NTH_a2 have similar bending stiffness, which are slightly higher than that of the C-NTH_a. For instance, the calculated bending stiffness is 1.63×10^{-27} N·m^2 and 3.79×10^{-27} N·m^2 for CN-NTH_a1 in the two vibration directions, respectively. Such results indicate that the presence of nitrogen atoms enhance the bending rigidity of the nanothreads. Specifically, the magnitude of the higher bending stiffness is over two times of the lower bending stiffness, signifying a strong anisotropic mechanical property in the lateral direction.

Of interest, Figure 8c also compares the bending stiffness of the nanothreads with other 1D carbon nanostructures. In literature, the reported bending stiffness for C-NTH ranges from 0.53×10^{-27} to 1.41×10^{-27} N·m2,[13, 28] which is uniformly below that of the examined CN-NTH. According to the theoretical calculations, the cumulene carbyne chain and polyyne carbyne chain have a bending stiffness around 8.5 and 6.7 eV·Å,[48] respectively, which is over an order of magnitude smaller than that of CN-NTH. However, comparing to the CNT, the bending stiffness of CN-NTH is much smaller, e.g., a (5,5) CNT has a much bending stiffness on the order of 10^5 kcal/mol·Å.[28] With the estimated bending stiffness, the persistence length L_p of the CN-NTH can be calculated. Following the concept in polymer physics,[49] can be estimated from $L_p = EI/k_BT$, where k_B is the Boltzmann constant and T is the temperature. The persistence length for CN-NTH_a1 and CN-NTH_a2 are found to be in the range of 393 nm to 915 nm and 403 nm to 958 nm at 300 K, respectively. These results indicate that a CN-NTH in the polymer I group shorter than ~400 nm behaves like a flexible elastic rod. For longer CN-NTH, its properties can only be described statistically.

4. Conclusion

Based on large-scale molecular dynamics simulations, we investigated the mechanical properties of the ultra-thin carbon nitride nanothreads (CN-NTHs). Comparing with the carbon nanothreads (C-NTHs), the presence of nitrogen atoms is found to enhance the tensile and bending stiffness of the nanothreads. Specifically, the CN-NTHs in the polymer I group and tube (3.0) group are found to possess a higher failure strain than their C-NTH counterparts. While, the CN-NTH in the polytwistane group has a smaller failure strain compared with the corresponding C-NTH. Simulation results show that the length of the C-C bonds is re-distributed due to the introduction of nitrogen atoms, which affect the stress or strain distribution during the tensile deformation. Based on the geometrical relationship, the C-C bonds and C-N bonds can be divided into different groups in C-NTHs and CN-NTHs. Within a same group, the C-N bonds are found to share a same changing tendency (either stretching or compressing) under the tensile deformation as the C-C bonds. Particularly, for the polymer I and tube (3,0) groups, the presence of nitrogen atoms introduces extra flexibility to the structure that delays the failure of the structure, i.e., resulting in a larger failure strain. However, in the polytwistane group, the existence of nitrogen atoms leads to earlier failure compared with the pristine structure. This study provides a comprehensive understanding of the mechanical properties of carbon nitride nanothreads, which should shed lights on their potential applications such as fibers or reinforcements for nanocomposites.

Supporting Information

The Supporting Information is available free of charge, including: bond group classifications of CN-NTHs and C-NTHs; bond distortion and extension during the tensile process; the trajectory of the centre of mass for CN-NTH_a1; and vibrational behaviours of CN-NTH_a2 and C-NTH_a.

AUTHOR INFORMATION

Corresponding Author

*E-mail: zhan.haifei@qut.edu.au; xuxu@jlu.edu.cn

Author Contributions

Z.Z. carried out the simulations. Z.Z., H.Z., Y.N., X.X., and Y.G. conducted the analysis and discussion.

Notes

There are no conflicts of interest to declare.

ACKNOWLEDGEMENT

Supports from the ARC Discovery Project (DP170102861) and National Natural Science Foundation of China (NNSFC, grant number 11372117) are gratefully acknowledged. This research was undertaken with the assistance of resource and services from Intersect Australia Ltd, and the National Computational Infrastructure (NCI), which is supported by Australian Government. This work was also supported by the Queensland University of Technology (QUT) through the use of their high-performance computing facilities. Z.Z. would like to acknowledge the financial support of China Scholarship Council (CSC) scholarship from Chinese government.

REFERENCES

1. Geim, A. K., Graphene: Status and Prospects. *Science* **2009**, *324*, 1530-1534.
2. Iijima, S., Helical Microtubules of Graphitic Carbon. *Nature* **1991**, *354*, 56.
3. Liu, J.; Rinzler, A. G.; Dai, H.; Hafner, J. H.; Bradley, R. K.; Boul, P. J.; Lu, A.; Iverson, T.; Shelimov, K.; Huffman, C. B., Fullerene Pipes. *Science* **1998**, *280*, 1253-1256.
4. Fitzgibbons, T. C.; Guthrie, M.; Xu, E.-s.; Crespi, V. H.; Davidowski, S. K.; Cody, G. D.; Alem, N.; Badding, J. V., Benzene-Derived Carbon Nanothreads. *Nat. Mater.* **2015**, *14*, 43.
5. Stojkovic, D.; Zhang, P.; Crespi, V. H., Smallest Nanotube: Breaking the Symmetry of Sp 3 Bonds in Tubular Geometries. *Phys. Rev. Lett.* **2001**, *87*, 125502.

6. Wen, X.-D.; Hoffmann, R.; Ashcroft, N., Benzene under High Pressure: A Story of Molecular Crystals Transforming to Saturated Networks, with a Possible Intermediate Metallic Phase. *J. Am. Chem. Soc.* **2011**, *133*, 9023-9035.

7. Olbrich, M.; Mayer, P.; Trauner, D., A Step toward Polytwistane: Synthesis and Characterization of C 2-Symmetric Tritwistane. *Org. Biomol. Chem.* **2014**, *12*, 108-112.

8. Xu, E.-s.; Lammert, P. E.; Crespi, V. H., Systematic Enumeration of Sp3 Nanothreads. *Nano Lett.* **2015**, *15*, 5124-5130.

9. Chen, B.; Hoffmann, R.; Ashcroft, N. W.; Badding, J.; Xu, E.; Crespi, V., Linearly Polymerized Benzene Arrays as Intermediates, Tracing Pathways to Carbon Nanothreads. *J. Am. Chem. Soc.* **2015**, *137*, 14373-14386.

10. Barua, S. R.; Quanz, H.; Olbrich, M.; Schreiner, P. R.; Trauner, D.; Allen, W. D., Polytwistane. *Chem.: Eur. J.* **2014**, *20*, 1638-1645.

11. Juhl, S. J.; Wang, T.; Vermilyea, B.; Li, X.; Crespi, V. H.; Badding, J. V.; Alem, N., Local Structure and Bonding of Carbon Nanothreads Probed by High-Resolution Transmission Electron Microscopy. *J. Am. Chem. Soc.* **2019**, *141*, 6937-6945.

12. Duan, P.; Li, X.; Wang, T.; Chen, B.; Juhl, S. J.; Koeplinger, D.; Crespi, V. H.; Badding, J. V.; Schmidt-Rohr, K., The Chemical Structure of Carbon Nanothreads Analyzed by Advanced Solid-State Nmr. *J. Am. Chem. Soc.* **2018**.

13. Zhan, H.; Zhang, G.; Bell, J. M.; Gu, Y., The Morphology and Temperature Dependent Tensile Properties of Diamond Nanothreads. *Carbon* **2016**, *107*, 304-309.

14. Feng, C.; Xu, J.; Zhang, Z.; Wu, J., Morphology-and Dehydrogenation-Controlled Mechanical Properties in Diamond Nanothreads. *Carbon* **2017**, *124*, 9-22.

15. Zhan, H.; Zhang, G.; Zhang, Y.; Tan, V. B. C.; Bell, J. M.; Gu, Y., Thermal Conductivity of a New Carbon Nanotube Analog: The Diamond Nanothread. *Carbon* **2016**, *98*, 232-237.

16. Zhan, H. F.; Gu, Y. T., Thermal Conduction of One-Dimensional Carbon Nanomaterials and Nanoarchitectures. *Chin. Phys. B* **2018**, *27*, 38103-038103.

17. Zhan, H.; Zhang, G.; Tan, V. B. C.; Gu, Y., The Best Features of Diamond Nanothread for Nanofibre Applications. *Nat. Commun.* **2017**, *8*, 14863.

18. Zhan, H.; Zhang, G.; Tan, V. B.; Cheng, Y.; Bell, J. M.; Zhang, Y. W.; Gu, Y., Diamond Nanothread as a New Reinforcement for Nanocomposites. *Adv. Funct. Mater.* **2016**, *26*, 5279-5283.

19. Duan, K.; Li, Y.; Li, L.; Hu, Y.; Wang, X., Diamond Nanothread Based Resonators: Ultrahigh Sensitivity and Low Dissipation. *Nanoscale* **2018**, *10*, 8058-8065.

20. Chen, B.; Wang, T.; Crespi, V. H.; Li, X.; Badding, J.; Hoffmann, R., All the Ways to Have Substituted Nanothreads. *J. Chem. Theory Comput.* **2018**, *14*, 1131-1140.

21. Silveira, J.; Muniz, A., Functionalized Diamond Nanothreads from Benzene Derivatives. *Phys. Chem. Chem. Phys.* **2017**, *19*, 7132-7137.

22. Nobrega, M. M.; Teixeira-Neto, E.; Cairns, A. B.; Temperini, M. L.; Bini, R., One-Dimensional Diamondoid Polyaniline-Like Nanothreads from Compressed Crystal Aniline. *Chem. Sci.* **2018**, *9*, 254-260.

23. Li, X., et al., Carbon Nitride Nanothread Crystals Derived from Pyridine. *J. Am. Chem. Soc.* **2018**, *140*, 4969-4972.

24. Demingos, P.; Muniz, A. R., Electronic and Mechanical Properties of Partially Saturated Carbon and Carbon Nitride Nanothreads. *J. Phys. Chem. C* **2019**.

25. Mattsson, T. R.; Lane, J. M. D.; Cochrane, K. R.; Desjarlais, M. P.; Thompson, A. P.; Pierce, F.; Grest, G. S., First-Principles and Classical Molecular Dynamics Simulation of Shocked Polymers. *Phys. Rev. B* **2010**, *81*, 054103.

26. Brenner, D. W.; Shenderova, O. A.; Harrison, J. A.; Stuart, S. J.; Ni, B.; Sinnott, S. B., A Second-Generation Reactive Empirical Bond Order (Rebo) Potential Energy Expression for Hydrocarbons. *J. Phys.: Condens. Matter* **2002**, *14*, 783.

27. Stuart, S. J.; Tutein, A. B.; Harrison, J. A., A Reactive Potential for Hydrocarbons with Intermolecular Interactions. *J. Chem. Phys.* **2000**, *112*, 6472-6486.

28. Roman, R. E.; Kwan, K.; Cranford, S. W., Mechanical Properties and Defect Sensitivity of Diamond Nanothreads. *Nano Lett.* **2015**, *15*, 1585-1590.

29. Ozden, S.; Machado, L. D.; Tiwary, C.; Autreto, P. A. S.; Vajtai, R.; Barrera, E. V.; Galvao, D. S.; Ajayan, P. M., Ballistic Fracturing of Carbon Nanotubes. *ACS Appl. Mater. Interfaces* **2016**, *8*, 24819-24825.

30. Yoon, K.; Ostadhossein, A.; van Duin, A. C., Atomistic-Scale Simulations of the Chemomechanical Behavior of Graphene under Nanoprojectile Impact. *Carbon* **2016**, *99*, 58-64.

31. Singh, S. K.; Srinivasan, S. G.; Neek-Amal, M.; Costamagna, S.; van Duin, A. C.; Peeters, F., Thermal Properties of Fluorinated Graphene. *Phys. Rev. B* **2013**, *87*, 104114.

32. Nosé, S., A Unified Formulation of the Constant Temperature Molecular Dynamics Methods. *J. Chem. Phys.* **1984**, *81*, 511-519.

33. Hoover, W. G., Canonical Dynamics: Equilibrium Phase-Space Distributions. *Phys. Rev. A* **1985**, *31*, 1695.

34. Plimpton, S., Fast Parallel Algorithms for Short-Range Molecular Dynamics. *J. Comput. Phys.* **1995**, *117*, 1-19.

35. Diao, J.; Gall, K.; Dunn, M. L., Atomistic Simulation of the Structure and Elastic Properties of Gold Nanowires. *J. Mech. Phys. Solids* **2004**, *52*, 1935-1962.

36. Silveira, J. F. R. V.; Muniz, A. R., First-Principles Calculation of the Mechanical Properties of Diamond Nanothreads. *Carbon* **2017**, *113*, 260-265.

37. Zhan, H.; Zhang, G.; Tan, V. B. C.; Cheng, Y.; Bell, J. M.; Zhang, Y.-W.; Gu, Y., From Brittle to Ductile: A Structure Dependent Ductility of Diamond Nanothread. *Nanoscale* **2016**, *8*, 11177-11184.

38. Silveira, J. F. R. V.; Muniz, A. R., Functionalized Diamond Nanothreads from Benzene Derivatives. *Phys. Chem. Chem. Phys.* **2017**, *19*, 7132-7137.

39. Zhan, H. F.; Gu, Y. T., A Fundamental Numerical and Theoretical Study for the Vibrational Properties of Nanowires. *J. Appl. Phys.* **2012**, *111*.

40. Zhan, H. F.; Gu, Y. T.; Park, H. S., Beat Phenomena in Metal Nanowires, and Their Implications for Resonance-Based Elastic Property Measurements. *Nanoscale* **2012**, *4*, 6779-6785.

41. Zheng, Z.; Zhan, H.; Nie, Y.; Bo, A.; Xu, X.; Gu, Y., General Existence of Flexural Mode Doublets in Nanowires Targeting Vectorial Sensing Applications. *Phys. Chem. Chem. Phys.* **2019**, *21*, 4136-4144.

42. Qin, Q.; Xu, F.; Cao, Y.; Ro, P. I.; Zhu, Y., Measuring True Young's Modulus of a Cantilevered Nanowire: Effect of Clamping on Resonance Frequency. *Small* **2012**.

43. Zhan, H. F.; Zhang, Y. Y.; Bell, J. M.; Zhang, B. C.; Gu, Y. T., Tailoring the Resonance of Bilayer Graphene Sheets by Interlayer Sp3 Bonds. *J. Phys. Chem. C* **2014**, *118*, 732-739.

44. Zhan, H. F.; Zhang, G. Y.; Zhang, B. C.; Bell, J. M.; Gu, Y. T., Tuning the Resonance Properties of 2d Carbon Nanotube Networks Towards a Mechanical Resonator. *Nanotechnology* **2015**, *26*, 315501.

45. Kim, S. Y.; Park, H. S., The Importance of Edge Effects on the Intrinsic Loss Mechanisms of Graphene Nanoresonators. *Nano Lett.* **2009**, *9*, 969-974.

46. Jiang, J.-W.; Park, H.; Rabczuk, T., Mos2 Nanoresonators: Intrinsically Better Than Graphene? *Nanoscale* **2014**, *6*, 3618.

47. Brigham, E. O.; Morrow, R., The Fast Fourier Transform. *IEEE Spectr.* **1967**, *4*, 63-70.

48. Liu, X.; Zhang, G.; Zhang, Y.-W., Tunable Mechanical and Thermal Properties of One-Dimensional Carbyne Chain: Phase Transition and Microscopic Dynamics. *J. Phys. Chem. C* **2015**, *119*, 24156-24164.

49. Doi, M.; Edwards, S., *The Theory of Polymer Dynamics Clarendon*; Oxford, 1986.

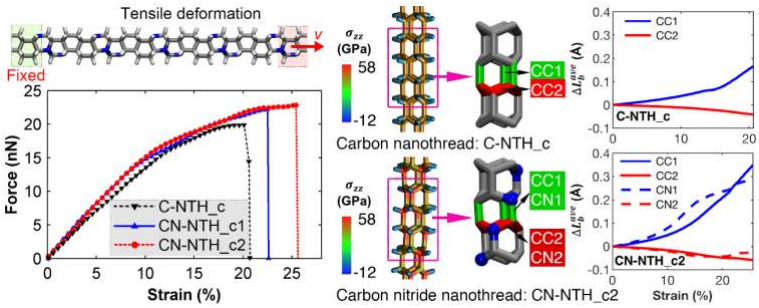
Tensile deformation
Fixed
V
Force (nN)
Strain (%)
C-NTH_c
CN-NTH_c1
CN-NTH_c2
σ_{zz} (GPa)
58
-12
Carbon nanothread: C-NTH_c
CC1
CC2
CN1
CN2
Carbon nitride nanothread: CN-NTH_c2
ΔL_b^{ave} (Å)
C-NTH_c
CN-NTH_c2

TOC Graphic